



# Photoprotective Effects of Oral Pterostilbene in UVB-Induced Skin Photoaging BALB/c Mouse Model

Raveena Vaidheswary Muralitharan<sup>1</sup>, Rana Ashraf Omar<sup>2</sup>, Jing Ren Poh<sup>2</sup>, Siti Fathiah Masre<sup>1</sup>, Dayang Fredalina Basri<sup>3</sup>, Ahmad Rohi Ghazali<sup>1,\*</sup>

<sup>1</sup> Center for Toxicology and Health Risk Studies (CORE), Faculty of Health Sciences, Universiti Kebangsaan Malaysia, Kuala Lumpur, Malaysia

<sup>2</sup> Biomedical Science Programme, Faculty of Health Sciences, Universiti Kebangsaan Malaysia, Kuala Lumpur, Malaysia

<sup>3</sup> Center for Diagnostic, Therapeutic and Investigative Studies (CODTIS), Faculty of Health Sciences, Universiti Kebangsaan Malaysia, Kuala Lumpur, Malaysia

\*Corresponding Author: Center for Toxicology and Health Risk Studies (CORE), Faculty of Health Sciences, Universiti Kebangsaan Malaysia, Kuala Lumpur, Malaysia.  
Email: rohi@ukm.edu.my

Received: 17 December, 2024; Revised: 18 January, 2025; Accepted: 29 January, 2025

## Abstract

**Background:** Photoaging results from prolonged and repeated exposure to solar ultraviolet-B (UVB) radiation. While sunscreen is effective in preventing ultraviolet (UV)-induced skin damage, oral antioxidants may offer additional protective benefits. Pterostilbene (PS), a compound found in blueberries and *Pterocarpus marsupium* heartwood, is recognized for its anti-aging and anti-photocarcinogenic properties. However, its photoprotective effects on photoaging have not been extensively studied.

**Objectives:** This study investigates the photoprotective effects of oral PS in a UVB-induced skin photoaging BALB/c mouse model.

**Methods:** Sixteen 7-week-old female BALB/c mice were randomly assigned to groups using an online random number generator. The mice received daily oral doses of corn oil or PS at 30 and 60 mg/kg in corn oil. After a 2-week period without UVB exposure, the UVB (-) group remained unexposed, while the UVB (+), UVB (+) PS30, and UVB (+) PS60 groups were subjected to increasing UVB doses three times a week for eight weeks, resulting in a cumulative exposure of 3.7 J/cm<sup>2</sup>. Weekly pinch tests were conducted throughout the 8-week exposure period. Photographs of the mice skin were taken before culling, and skin samples were collected for Hematoxylin & Eosin (H&E) staining, Masson's trichrome staining, reduced glutathione (GSH) assay, and melanin content assay.

**Results:** The UVB (+) PS30 group showed reduced erythema and wrinkles, while the PS60 group exhibited the most significant improvement in photoaged skin, with eliminated erythema, reduced wrinkles, and smoother skin. The PS30 (4.05 ± 0.11 seconds) and PS60 (3.65 ± 0.06 seconds) groups significantly reduced pinch test times compared to the UVB (+) group (4.96 ± 0.12 seconds), indicating improved skin elasticity. Additionally, PS30 (61.87 ± 3.58 μm) and PS60 (43.64 ± 2.08 μm) significantly reduced epidermal thickness compared to the UVB (+) group (67.39 ± 1.69 μm). Collagen content significantly increased in the PS30 (1.41 ± 0.04) and PS60 (1.27 ± 0.02) groups compared to the UVB (+) group (1.11 ± 0.01). The GSH levels (μmol/mg) were significantly higher in the PS30 (0.56 ± 0.01) and PS60 (0.56 ± 0.02) groups compared to the UVB (+) group (0.48 ± 0.01), with no significant difference between the PS doses. Melanin content (μmol/mg) in the PS30 (0.34 ± 0.01) and PS60 (0.35 ± 0.01) groups showed no significant difference compared to the UVB (+) group (0.387 ± 0.04).

**Conclusions:** Oral PS demonstrated significant photoprotective effects in UVB-induced skin photoaging, suggesting its potential as an anti-photoaging agent in the cosmeceutical and nutraceutical industries.

**Keywords:** Oral, Pterostilbene, UVB, Skin, Photoaging

## 1. Background

The skin possesses inherent protective mechanisms against aging, which diminish with advancing age (1-3). Solar ultraviolet (UV) radiation is responsible for approximately 80% of skin damage, significantly contributing to skin cancer and aging (4). The UVA radiation generates reactive oxygen species (ROS), leading to indirect DNA damage. In contrast, ultraviolet-B (UVB) radiation is a major factor in skin damage due to its ability to generate intracellular ROS (5-7), directly damaging DNA and triggering inflammation. The UVB photons are 1000 times more energetic than UVA

photons, making UVB the primary cause of sunburn, tanning, and photocarcinogenesis (7, 8). Chronic UV exposure results in photoaging, characterized by wrinkles, roughness, loss of skin tensile strength, fragility, dyspigmentation, and dryness (1, 9-11). Photoaging is also a precursor to photocarcinogenesis.

Skin photoprotection involves both topical formulations and oral supplements (4). While sunscreen is commonly used, it requires frequent reapplication, often leading to inadequate protection. Conversely, oral supplements can repair damage in the deeper skin layers, making exogenous antioxidants in oral supplements more beneficial and practical (12, 13).

This study focuses on pterostilbene (PS), an active compound found in blueberries and *Pterocarpus marsupium* heartwood (14), known for its anti-aging and anti-photocarcinogenic properties (15, 16). Notably, orally administered PS has higher bioavailability and a longer half-life compared to its analogue, resveratrol (17, 18).

## 2. Objectives

Therefore, this study aims to investigate the photoprotective effects of oral PS in a UVB-induced skin photoaging BALB/c mouse model. The animal model was selected to mimic human photoaging, providing controlled conditions to explore therapeutic interventions.

## 3. Methods

### 3.1. Sample Size Calculation

The number of mice required for the study was calculated using the resource equation approach (19). Based on this calculation, 4 mice per group were needed to maintain a degree of freedom (DF) of 10. The sample size was further adjusted to account for an expected attrition rate of 10% (20), confirming that 4 mice per group were sufficient.

### 3.2. Animal Maintenance and Experimentation

Sixteen female BALB/c mice, aged six weeks, were procured from the Faculty of Science and Technology animal house at Universiti Kebangsaan Malaysia (UKM) and housed under standard laboratory conditions, which included consistent temperature, humidity, and lighting, at the Faculty of Health Sciences animal house, UKM. The mice were fed standard mouse pellets with water provided ad libitum. Inclusion criteria required healthy mice that met the study requirements, while exclusion criteria included mice exhibiting unrelated illnesses, infections, or skin lesions. Experimental conditions and treatment protocols were standardized to ensure consistency. Ethical approval was obtained from the UKM Animal Ethics Committee (UKMAEC), with the approval code: FSK/2020/AHMAD ROHI/25-NOV./1138-DEC.-2020-AUG.-2022. This study adheres to the ARRIVE guidelines for reporting animal research (21), with a completed ARRIVE guidelines 2.0 checklist available in Appendix 1 in Supplementary File.

### 3.3. Reagents

The following materials were used in the study:

Pterostilbene (J&K Scientific, USA), corn oil (Mazola®, USA), 37% formaldehyde (R&M Chemicals, United Kingdom), sodium phosphate dibasic (Na<sub>2</sub>HPO<sub>4</sub>) (Amresco, USA), sodium phosphate monobasic (NaH<sub>2</sub>PO<sub>4</sub>) (Merck, Germany), 99.8% absolute ethanol (Chemiz, Malaysia), xylene (Chemiz, Malaysia), paraffin wax (Sigma-Aldrich, USA), Harris hematoxylin powder (Sigma-Aldrich, USA), potassium aluminium sulphate (Sigma-Aldrich, Germany), mercury (II) oxide red (Merck, Germany), glacial acetic acid (Chemiz, Malaysia), eosin Y powder (Sigma-Aldrich, USA), 37% hydrochloric acid (R&M Chemicals, United Kingdom), Bouin's solution (Chemiz, Malaysia), Biebrich scarlet sodium salt (Sigma-Aldrich, Germany), acid fuchsin (Sigma-Aldrich, Germany), Weigert's iron hematoxylin kit (Merck, Germany), aniline blue diammonium salt (Sigma-Aldrich, Germany), phosphotungstic acid hydrate (Sigma-Aldrich, Germany), phosphomolybdic acid hydrate (Sigma-Aldrich, Germany), dibutylphthalate polystyrene xylene (DPX) (Sigma-Aldrich, USA), phosphate buffered saline (PBS) tablets (Oxoid, United Kingdom), Coomassie Blue G-250 (Fisher Scientific, USA), 85% phosphoric acid (Chemiz, Malaysia), bovine serum albumin (Nacalai Tesque, Japan), L-glutathione (GSH) reduced (Sigma-Aldrich, USA), 5,5'-Dithiobis(2-nitrobenzoic acid) (DTNB) (Sigma-Aldrich, USA), ethylenediaminetetraacetic acid (EDTA) powder (Chemiz, Malaysia), metaphosphoric acid (Merck, Germany), synthetic melanin (Sigma-Aldrich, USA), sodium hydroxide (Merck, Germany), chloroform (Merck, Germany), and phenol (Merck, Germany). All chemicals were of analytical grade and commercially produced.

### 3.4. Experimental Design

After a 1-week acclimatization period, the mice were divided into four groups of four mice each (n = 4, with each mouse regarded as an experimental unit). The allocation of mice into each group was conducted using an online random number generator (<https://www.graphpad.com/quickcalcs/randomize1/>) to generate the randomization sequence. The groups were as follows: Ultraviolet-B (-) as a negative control, UVB (+) as a vehicle control, UVB (+) PS30 (30 mg/kg low-dose PS), and UVB (+) PS60 (60 mg/kg high-dose PS). A positive control group was not included in this study due to the absence of a widely accepted gold standard for oral photoprotection (12). Unlike topical photoprotection, where tretinoin is currently the gold standard for treating photoaging (22), oral approaches remain under exploration. Therefore, comparisons were made with

**Table 1.** Ultraviolet-B Dose Exposure Plan

Groups	Weeks									
	1	2	3	4	5	6	7	8	9	10
UVB (-)	-	-	-	-	-	-	-	-	-	-
UVB (+) <sup>a</sup>	-	-	48+	67+	112+	133+	165+	184+	213+	237+
UVB (+) PS30	-	-	48+	86+	112+	156+	165+	200+	213+	250+
UVB (+) PS60	-	-	67	86	133	156	184	200	237	250

Abbreviation: UVB, ultraviolet-B.

<sup>a</sup> Unit: mJ/cm<sup>2</sup>.

the negative control and vehicle control groups to establish a relative baseline for efficacy.

For two weeks, daily oral gavage was administered without UVB exposure. Mice were fasted for four hours from food before gavage, with volumes set at 0.5% of body weight. The UVB (-) and UVB (+) groups received corn oil, while the UVB (+) PS30 and UVB (+) PS60 groups received PS in corn oil, respectively. After two weeks, a 2.5 × 5 cm area of dorsal fur was shaved clean. Daily oral gavage continued for the next eight weeks, with UVB exposure applied only to the UVB (+), PS30, and PS60 groups.

### 3.5. Ultraviolet-B Dose Exposure Plan

Photoaging was induced in the mice by exposing them to UVB irradiation using a 15-watt lamp (UVP, USA) that emitted UV light at 312 nm. The irradiation intensity was measured using a UVP UVX radiometer (Analytik Jena, Germany). The dose of UVB exposure was calculated using the following formula (23):

$$UV \text{ dose } (mJ/cm^2) = \text{Fluence rate } (mW/cm^2) \times \text{Irradiation time } (seconds)$$

The UVB dose exposure plan, as outlined in Table 1, was adapted from Saito et al. (24). Only the UVB (+), PS30, and PS60 groups were exposed to UVB irradiation three times a week with increasing doses, starting from Week 3 and concluding at Week 10, resulting in a cumulative total of 3702 mJ/cm<sup>2</sup> or 3.702 J/cm<sup>2</sup>. Prior to UVB irradiation, the mice were anesthetized with 0.1 mL/50 g of KTX (a mixture of ketamine, xylazine, tiletamine, and zolazepam) and had their eyes covered with a black polyester waterproof fabric to prevent UVB damage.

### 3.6. Macroscopic Evaluation of Photoaging

Pinch tests (25, 26) were conducted once a week throughout the 8-week irradiation period. Mice were anesthetized using KTX (0.1 mL/50 g) before pinching

and stretching the skin at the midline of the dorsal area. The time taken (in seconds) for the mice skin to recover to its normal conformation was recorded. Each week, the pinch test was performed four times per mouse.

Upon completion of the treatment, mice were placed under deep anesthesia with a KTX overdose, and photographs of the dorsal skin were taken. Subsequently, the mice were euthanized by cervical dislocation. By first suppressing central nervous system activity with KTX to induce immobilization, cervical dislocation was performed swiftly and effectively, ensuring minimal pain and distress for the mice. The dorsal skin was harvested and divided into equal parts for histopathological observation (the primary outcome measure) and biochemical analyses.

Blinding was not feasible due to visible photoaging effects on the mice's skin, such as thickening, erythema, peeling, and wrinkles. However, other outcome measures, such as histology and biochemical analyses, were objective and quantifiable, reducing the risk of bias. An independent external reviewer was also consulted to validate our findings and further reduce bias.

### 3.7. Histological Analyses

The harvested dorsal skin was fixed in 10% neutral buffered formalin, processed, embedded in paraffin, and sectioned at 5 μm. Hematoxylin & Eosin (H&E) staining was employed to assess histological features of photoaging, which include changes in the epidermis and dermis, as well as the infiltration of inflammatory cells. Epidermal thickness was measured using Fiji v 2.15.0. Masson's trichrome staining (27) was utilized to evaluate collagen content, which was quantified using color deconvolution in Fiji v 2.15.0.

For the measurement of epidermal thickness, the four best images were selected to represent each mouse, and each image was measured four times at different areas across the epidermis. Similarly, the four best

images were chosen for collagen content quantification to represent each mouse.

### 3.8. Skin Tissue Homogenization

The harvested dorsal skin was washed with cold phosphate-buffered saline (PBS), snap-frozen in liquid nitrogen, and stored at  $-80^{\circ}\text{C}$ . After weighing and finely chopping, the skin was homogenized in cold sodium phosphate buffer (pH 6.8). The homogenate was then centrifuged at 8000 rpm for 20 minutes at  $4^{\circ}\text{C}$ , and the supernatant was stored at  $-80^{\circ}\text{C}$  for subsequent GSH and melanin content assays.

### 3.9. Glutathione Assay

Before conducting the assay, the protein concentration of the skin supernatant was determined using the Bradford method (28). The GSH assay, a measure of endogenous antioxidants, was performed using the Ellman method (29). Initially, 50  $\mu\text{L}$  of a 5% metaphosphoric acid solution was mixed with 50  $\mu\text{L}$  of the supernatant. The mixture was vortexed and centrifuged at 3000 rpm for 10 minutes at  $4^{\circ}\text{C}$ . The resulting supernatant was then used for the GSH assay.

Subsequently, 30  $\mu\text{L}$  of reaction buffer solution (containing sodium phosphate dibasic, EDTA, and distilled water, at pH 8.0) was added to the wells, followed by 50  $\mu\text{L}$  of supernatant into each corresponding well. Then, 10  $\mu\text{L}$  of DTNB solution was added to all wells, and the microplate was incubated at room temperature for 15 minutes in the dark. Absorbance was read at 412 nm. The concentration of GSH was determined by substituting the absorbance value into the equation of the GSH standard curve. Four technical replicates per mouse were performed. The final GSH concentration was calculated as shown below and expressed as  $\mu\text{mol}/\text{mg}$ :

$$\begin{aligned} \text{GSH concentration } (\mu\text{mol}/\text{mg}) \\ = \text{GSH (mM)} / \text{Total protein (mg/mL)} \end{aligned}$$

### 3.10. Melanin Content Assay

Skin melanin content was determined using a modified method by Iwata et al. (30). Approximately 350  $\mu\text{L}$  of skin homogenate was mixed with 2N sodium hydroxide and incubated for two days at  $60^{\circ}\text{C}$  to solubilize melanin. Subsequently, an equal volume of distilled water was added to the homogenate, followed by the addition of 700  $\mu\text{L}$  of a chloroform:Phenol (1:1) mixture. This mixture was vortexed and centrifuged at  $5000 \times g$  for 10 minutes to separate the phases. The resulting supernatant was measured at 400 nm using a

microplate reader. The obtained values were expressed as micrograms of melanin per milligram wet weight of skin ( $\mu\text{g}$  melanin/mg) (31). Four technical replicates per mouse were performed. The standard curve was generated similarly, using 25  $\mu\text{g}/\text{mL}$  of synthetic melanin instead of homogenate.

### 3.11. Statistical Analysis

Data were analyzed using GraphPad Prism v8.3.0 and are presented as mean  $\pm$  standard error of the mean (SEM) for quantitative analysis. Normality was confirmed with the Shapiro-Wilk test, validating the use of one-way ANOVA for group comparisons. Statistical significance was set at  $P < 0.05$ . All mice ( $n = 4$  per group) were included in all analyses, with no exclusions.

## 4. Results

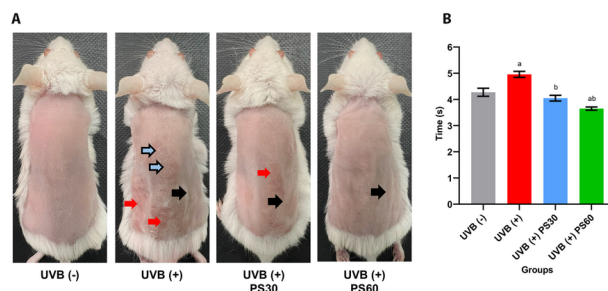
### 4.1. Effect of Ultraviolet-B Irradiation and Pterostilbene on Skin Macroscopic Appearance and Elasticity

Figure 1A illustrates the macroscopic appearance of the mice's skin after the experiment. The UVB (-) group exhibited fine wrinkles without redness, whereas the UVB (+) group displayed coarse wrinkles, erythema, and peeling. Pterostilbene treatment improved the appearance of photoaged skin: The UVB (+) PS30 group showed reduced erythema and coarse wrinkles, while the UVB (+) PS60 group eliminated erythema and resulted in smoother skin, although some coarse wrinkles remained.

In Figure 1B, the pinch test results indicated that the UVB (+) group took significantly longer ( $4.957 \pm 0.115$  seconds,  $P < 0.01$ ) to return to its normal skin conformation compared to the UVB (-) group ( $4.275 \pm 0.154$  seconds), suggesting reduced elasticity. Pterostilbene significantly improved skin elasticity ( $P < 0.0001$ ), as evidenced by the reduced time in the UVB (+) PS30 group ( $4.049 \pm 0.109$  seconds) and the UVB (+) PS60 group ( $3.650 \pm 0.062$  seconds) compared to the UVB (+) group. Although there was no significant difference between the PS30 and PS60 groups ( $P > 0.05$ ), the PS60 group showed a further reduction in time below the UVB (-) levels ( $P < 0.01$ ), demonstrating the greatest improvement in elasticity.

### 4.2. Skin Histopathological Changes of Ultraviolet-B Irradiation and Pterostilbene Treatment

Figure 2A illustrates increased epidermal thickness and inflammatory cell infiltration in the UVB (+) group compared to the UVB (-) group. The UVB (+) PS30 and UVB (+) PS60 groups demonstrated reduced epidermal



**Figure 1.** A, Skin macroscopic appearance. The arrows indicate (black) coarse wrinkles, (red) skin erythema and (blue) skin peeling; B, Skin recovery time via pinch test. [a = significant vs. ultraviolet-B (UVB) (-), b = significant vs. UVB (+)].

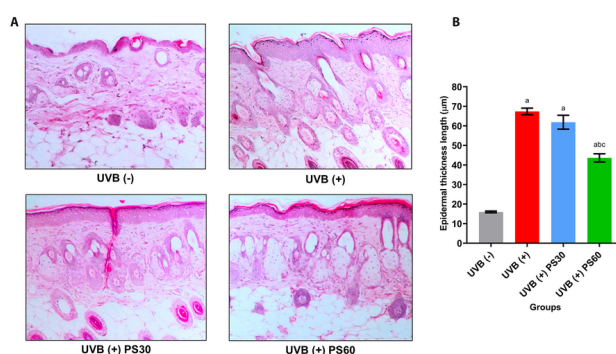


**Figure 2.** A, Hematoxylin & Eosin (H&E) staining of skin at 10x magnification; B, Epidermal thickness length. [a = significant vs. Ultraviolet-B (UVB) (-), b = significant vs. UVB (+), c = significant vs. UVB (+) PS30].

thickness, although inflammation persisted. **Figure 2B** confirms a significant increase in thickness for the UVB (+) group ( $67.388 \pm 1.688 \mu\text{m}$ ,  $P < 0.0001$ ) compared to the UVB (-) group ( $15.993 \pm 0.441 \mu\text{m}$ ). The UVB (+) PS60 group significantly reduced thickness ( $43.640 \pm 2.080 \mu\text{m}$ ) compared to both the UVB (+) group ( $P < 0.0001$ ) and the UVB (+) PS30 group ( $61.869 \pm 3.577 \mu\text{m}$ ,  $P < 0.001$ ), indicating that PS60 provided the greatest improvement.

**Figure 3A** highlights collagen content (blue), which is quantified in **Figure 3B**. The UVB (+) group ( $1.105 \pm 0.013$ ) showed a slight, non-significant increase in collagen compared to the UVB (-) group ( $1.000 \pm 0.026$ ,  $P > 0.05$ ). Pterostilbene significantly increased collagen in the UVB (+) PS30 group ( $1.407 \pm 0.040$ ,  $p < 0.0001$ ) and the UVB (+) PS60 group ( $1.266 \pm 0.020$ ,  $P < 0.01$ ) when compared to the UVB (+) group. However, the PS30 group showed a greater increase than the PS60 group ( $P < 0.05$ ),

suggesting that PS30 was more effective at boosting collagen content.

#### 4.3. Effect of Ultraviolet-B Irradiation and Pterostilbene on Skin Glutathione and Melanin

**Figure 4A** demonstrates a significant decrease in GSH levels in the UVB (+) group ( $0.477 \pm 0.014 \mu\text{mol/mg}$ ,  $P < 0.01$ ) compared to the UVB (-) group ( $0.556 \pm 0.010 \mu\text{mol/mg}$ ). Pterostilbene treatment significantly increased GSH levels in the UVB (+) PS30 group ( $0.564 \pm 0.011 \mu\text{mol/mg}$ ) and the UVB (+) PS60 group ( $0.563 \pm 0.018 \mu\text{mol/mg}$ ) when compared to the UVB (+) group ( $P < 0.01$ ), with no significant difference between the doses ( $P > 0.05$ ).

In **Figure 4B**, the UVB (+) group ( $0.387 \pm 0.042 \mu\text{g/mg}$ ) showed a significant increase in melanin content compared to the UVB (-) group ( $0.271 \pm 0.005 \mu\text{g/mg}$ ,  $P < 0.05$ ). The UVB (+) PS30 group ( $0.337 \pm 0.007 \mu\text{g/mg}$ ) and

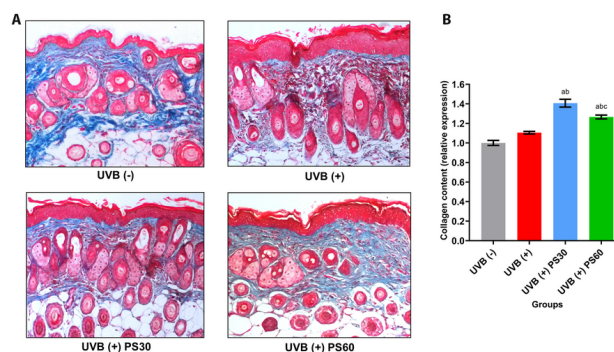


**Figure 3.** A, Masson's trichrome staining of skin at 10x magnification; B, relative expression of collagen content. [a = significant vs. ultraviolet-B (UVB) (-), b = significant vs. UVB (+), c = significant vs. UVB (+) PS30].

the UVB (+) PS60 group ( $0.347 \pm 0.008 \mu\text{g}/\text{mg}$ ) showed no significant difference ( $P > 0.05$ ) compared to other groups, indicating that PS had no effect on melanin levels in photoaged skin.

## 5. Discussion

Only one in vivo study has demonstrated that topical PS is more effective than resveratrol against UVB-induced photoaging (32). To date, no studies have investigated the effects of oral PS in preventing photoaging. In our study, the UVB (+) PS60 group exhibited smooth skin with no redness and only coarse wrinkles, while the UVB (+) group showed significant UVB-induced damage. Pterostilbene mitigated UVB-induced oxidative stress and preserved skin integrity, unlike the UVB (+) group, where endogenous skin antioxidants alone were insufficient to prevent damage.

The pinch test revealed that the UVB (+) PS60 group demonstrated improved elasticity, as evidenced by faster skin recovery time compared to both the UVB (+) and UVB (-) groups. This suggests that PS at a higher dose restored elasticity more effectively than untreated skin.

Hematoxylin & Eosin staining showed significant epidermal thickening in the UVB (+) group. This thickening is attributed to UV irradiation, which causes sunburnt cells (apoptotic keratinocytes), followed by increased cell division to replace lost cells, temporarily thickening the epidermis to shield basal stem cells. However, chronic UV exposure may eventually deplete stem cells, leading to atrophy (8). In our study, the UVB (+) PS60 group significantly decreased epidermal thickness compared to the UVB (+) and UVB (+) PS30 groups, demonstrating its superior ability to ameliorate photoaging-induced epidermal thickening.

Masson's Trichrome staining indicated a slight, non-significant increase in collagen in the UVB (+) group, possibly as a photoprotective mechanism before collagen degradation or due to UV-induced collagen cross-linking (33). Interestingly, the UVB (+) PS30 group exhibited significantly higher collagen density than the UVB (+) PS60 group. This finding parallels a clinical study (34) where high-dose beta-carotene exhibited pro-oxidant effects, whereas a low dose demonstrated antioxidant properties. However, further investigations are needed to confirm the specific effects of PS on collagen.

Reduced GSH is a ubiquitous antioxidant that counteracts the oxidizing effects of reactive species (35, 36). In the UVB (+) group, GSH levels significantly decreased compared to the UVB (-) group, likely due to the need to counteract ROS from UV exposure. In contrast, GSH levels in both PS-treated groups were restored to levels similar to the UVB (-) group. Despite this, no significant difference between the doses was observed, indicating that either dose could have a beneficial effect.

Finally, melanin content was significantly increased in the UVB (+) group compared to the UVB (-) group. Increased melanin synthesis is vital for skin photoprotection (37, 38). However, melanin can also increase intracellular ROS, which causes DNA damage and p53 activation (39, 40). Hence, antioxidants are crucial to counter the ROS produced. In this study, both PS doses showed a non-significant decreasing trend in melanin, suggesting that higher doses may be required for notable effects.

There are several limitations in our study. First, pinch test results should be paired with an objective

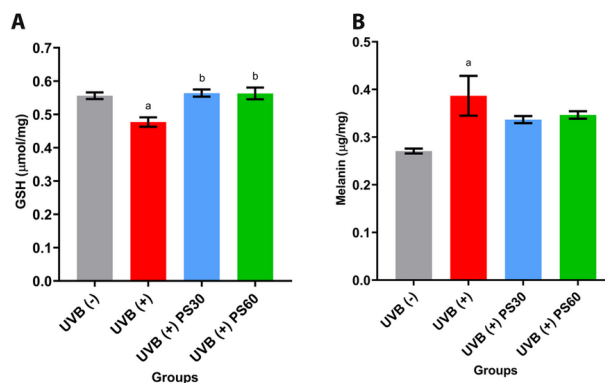


**Figure 4.** A, Skin glutathione (GSH) level; B, skin melanin content. [a = significant vs. ultraviolet-B (UVB) (-), b = significant vs. UVB (+)].

measurement of elastin to further reduce bias. Additionally, investigating other antioxidants, such as superoxide dismutase and GSH peroxidase, would broaden the understanding of PS's antioxidant profile. Finally, pairing melanin results with tyrosinase measurement would better elucidate PS's role in melanogenesis.

### 5.1. Conclusions

Overall, our study highlights the potential of oral PS to combat oxidative stress and complement topical treatments to mitigate photoaging. In UVB-induced skin photoaging, oral PS exhibited significant photoprotective properties. Notably, 60 mg/kg PS proved most effective in enhancing skin appearance and elasticity as well as reducing epidermal thickness, while 30 mg/kg was best at increasing collagen content. Both doses successfully restored GSH levels. However, neither dose significantly reduced melanin.

### Acknowledgements

This research is supported by the Research University Grant (GUP-2020-053), Universiti Kebangsaan Malaysia (UKM).

### Supplementary Material

Supplementary material(s) is available [here](#) [To read supplementary materials, please refer to the journal website and open PDF/HTML].

### Footnotes

**Authors' Contribution:** Study concept and design: R. V. M. and A. R. G.; Acquisition of data: R. V. M., R. A. O., and J. R. P.; Analysis and interpretation of data: R. V. M., R. A. O., and J. R. P.; Drafting of the manuscript: R. V. M.; Critical revision of the manuscript for important intellectual content: S. F. M., D. F. B., and A. R. G.; Statistical analysis: R. V. M., R. A. O., and J. R. P.; Administrative, technical, and material support: A. R. G.; Study supervision: S. F. M., D. F. B., and A. R. G.

**Conflict of Interests Statement:** The authors declared no conflict of interests.

**Data Availability:** The dataset presented in the study is available on request from the corresponding author during submission or after publication. The data are not publicly available due to institutional policies, but will be made available upon reasonable request.

**Ethical Approval:** Ethical approval was obtained from the Universiti Kebangsaan Malaysia (UKM) Animal Ethics Committee (UKMAEC), with code: FSK/2020/AHMAD ROHI/25-NOV./1138-DEC.-2020-AUG.-2022.

**Funding/Support:** This research is supported by the Research University Grant (GUP-2020-053), Universiti Kebangsaan Malaysia (UKM).

### References

1. Veysey EC, Finlay AY. Aging and the Skin. *Brocklehurst's Textbook of Geriatric Medicine and Gerontology*. Elsevier; 2010. p. 133-7. <https://doi.org/10.1016/b978-1-4160-6231-8.10022-4>.
2. Shin SH, Lee YH, Rho NK, Park KY. Skin aging from mechanisms to interventions: focusing on dermal aging. *Front Physiol*. 2023;14:1195272. [PubMed ID: 37234413]. [PubMed Central ID: PMC10206231]. <https://doi.org/10.3389/fphys.2023.1195272>.

3. Zhang M, Lin Y, Han Z, Huang X, Zhou S, Wang S, et al. Exploring mechanisms of skin aging: insights for clinical treatment. *Front Immunol*. 2024;**15**:1421858. [PubMed ID: 39582871]. [PubMed Central ID: PMC1581952]. <https://doi.org/10.3389/fimmu.2024.1421858>.
4. Poljsak B, Dahmane R. Free radicals and extrinsic skin aging. *Dermatol Res Pract*. 2012;**2012**:135206. [PubMed ID: 22505880]. [PubMed Central ID: PMC3299230]. <https://doi.org/10.1155/2012/135206>.
5. Choi HJ, Alam MB, Baek ME, Kwon YG, Lim JY, Lee SH. Protection against UVB-Induced Photoaging by *Nyssa fruticans* via Inhibition of MAPK/AP-1/MMP-1 Signaling. *Oxid Med Cell Longev*. 2020;**2020**:2905362. [PubMed ID: 32685089]. [PubMed Central ID: PMC7330638]. <https://doi.org/10.1155/2020/2905362>.
6. Petruk G, Raiola A, Del Giudice R, Barone A, Frusciantone L, Rigano MM, et al. An ascorbic acid-enriched tomato genotype to fight UVA-induced oxidative stress in normal human keratinocytes. *J Photochem Photobiol B*. 2016;**163**:284-9. [PubMed ID: 27599115]. <https://doi.org/10.1016/j.jphotobiol.2016.08.047>.
7. Al-Sadek T, Yusuf N. Ultraviolet Radiation Biological and Medical Implications. *Curr Issues Mol Biol*. 2024;**46**(3):1924-42. [PubMed ID: 38534742]. [PubMed Central ID: PMC10968857]. <https://doi.org/10.3390/cimb46030126>.
8. Gilchrist BA. Photoaging. *J Invest Dermatol*. 2013;**133**(E1):E2-6. [PubMed ID: 23820721]. <https://doi.org/10.1038/skinbio.2013.176>.
9. Wlaschek M, Tantcheva-Poor I, Naderi L, Ma W, Schneider LA, Razi-Wolf Z, et al. Solar UV irradiation and dermal photoaging. *J Photochem Photobiol B*. 2001;**63**(1-3):41-51. [PubMed ID: 11684450]. [https://doi.org/10.1016/s1011-1344\(01\)00201-9](https://doi.org/10.1016/s1011-1344(01)00201-9).
10. Chen CC, Chiang AN, Liu HN, Chang YT. EGB-761 prevents ultraviolet B-induced photoaging via inactivation of mitogen-activated protein kinases and proinflammatory cytokine expression. *J Dermatol Sci*. 2014;**75**(1):55-62. [PubMed ID: 24802711]. <https://doi.org/10.1016/j.jdermsci.2014.04.001>.
11. Xiong J, Wang F, Yang Y, Yang Y, Liu Z. Preventive effect of human umbilical cord mesenchymal stem cells on skin aging in rats. *Heliyon*. 2024;**10**(2). e24342. [PubMed ID: 38293418]. [PubMed Central ID: PMC10826728]. <https://doi.org/10.1016/j.heliyon.2024.e24342>.
12. Parrado C, Philips N, Gilaberte Y, Juarranz A, Gonzalez S. Oral Photoprotection: Effective Agents and Potential Candidates. *Front Med (Lausanne)*. 2018;**5**:188. [PubMed ID: 29998107]. [PubMed Central ID: PMC6028556]. <https://doi.org/10.3389/fmed.2018.00188>.
13. Calvo MJ, Navarro C, Duran P, Galan-Freyre NJ, Parra Hernandez LA, Pacheco-Londono LC, et al. Antioxidants in Photoaging: From Molecular Insights to Clinical Applications. *Int J Mol Sci*. 2024;**25**(4). [PubMed ID: 38397077]. [PubMed Central ID: PMC10889126]. <https://doi.org/10.3390/ijms25042403>.
14. McCormack D, McFadden D. A review of pterostilbene antioxidant activity and disease modification. *Oxid Med Cell Longev*. 2013;**2013**:575482. [PubMed ID: 23691264]. [PubMed Central ID: PMC3649683]. <https://doi.org/10.1155/2013/575482>.
15. Li YR, Li S, Lin CC. Effect of resveratrol and pterostilbene on aging and longevity. *Biofactors*. 2018;**44**(1):69-82. [PubMed ID: 29210129]. <https://doi.org/10.1002/biof.1400>.
16. Shelan Nagapan T, Rohi Ghazali A, Fredalina Basri D, Nallance Lim W. Photoprotective Effect Of Stilbenes And Its Derivatives against Ultraviolet Radiation-Induced Skin Disorders. *Biomed Pharmacol J*. 2018;**11**(3):199-208. <https://doi.org/10.13005/bpj/1481>.
17. Kapetanovic IM, Muzzio M, Huang Z, Thompson TN, McCormick DL. Pharmacokinetics, oral bioavailability, and metabolic profile of resveratrol and its dimethylether analog, pterostilbene, in rats. *Cancer Chemother Pharmacol*. 2011;**68**(3):593-601. [PubMed ID: 21116625]. [PubMed Central ID: PMC3090701]. <https://doi.org/10.1007/s00280-010-1525-4>.
18. Liu P, Tang W, Xiang K, Li G. Pterostilbene in the treatment of inflammatory and oncological diseases. *Front Pharmacol*. 2023;**14**:1323377. [PubMed ID: 38259272]. [PubMed Central ID: PMC10800393]. <https://doi.org/10.3389/fphar.2023.1323377>.
19. Arifin WN, Zahiruddin WM. Sample Size Calculation in Animal Studies Using Resource Equation Approach. *Malays J Med Sci*. 2017;**24**(5):101-5. [PubMed ID: 29386977]. [PubMed Central ID: PMC5772820]. <https://doi.org/10.21315/mjms2017.24.5.11>.
20. Charan J, Kantharia ND. How to calculate sample size in animal studies? *J Pharmacol Pharmacother*. 2013;**4**(4):303-6. [PubMed ID: 24250214]. [PubMed Central ID: PMC3826013]. <https://doi.org/10.4103/0976-500X.119726>.
21. Percie du Sert N, Hurst V, Ahluwalia A, Alam S, Avey MT, Baker M, et al. The ARRIVE guidelines 2.0: Updated guidelines for reporting animal research. *PLoS Biol*. 2020;**18**(7). e3000410. [PubMed ID: 32663219]. [PubMed Central ID: PMC7360023]. <https://doi.org/10.1371/journal.pbio.3000410>.
22. Siddiqui Z, Zufall A, Nash M, Rao D, Hirani R, Russo M. Comparing Tretinoin to Other Topical Therapies in the Treatment of Skin Photoaging: A Systematic Review. *Am J Clin Dermatol*. 2024;**25**(6):873-90. [PubMed ID: 39348007]. <https://doi.org/10.1007/s40257-024-00893-w>.
23. Bolton JR. Calculation of ultraviolet fluence rate distributions in an annular reactor: significance of refraction and reflection. *Water Res*. 2000;**34**(13):3315-24. [https://doi.org/10.1016/s0043-1354\(00\)00087-7](https://doi.org/10.1016/s0043-1354(00)00087-7).
24. Saito M, Tanaka M, Misawa E, Yao R, Nabeshima K, Yamauchi K, et al. Oral administration of Aloe vera gel powder prevents UVB-induced decrease in skin elasticity via suppression of overexpression of MMPs in hairless mice. *Biosci Biotechnol Biochem*. 2016;**80**(7):1416-24. [PubMed ID: 27045316]. <https://doi.org/10.1080/09168451.2016.1156480>.
25. Tsukahara K, Moriwaki S, Hotta M, Fujimura T, Sugiyama-Nakagiri Y, Sugawara S, et al. The effect of sunscreen on skin elastase activity induced by ultraviolet-A irradiation. *Biol Pharm Bull*. 2005;**28**(12):2302-7. [PubMed ID: 16327169]. <https://doi.org/10.1248/bpb.28.2302>.
26. Lin X, Fan Y, Li L, Chen J, Huang S, Yue W, et al. The Protective Effects of Silkworm (*Bombyx mori*) Pupae Peptides on UV-Induced Skin Photoaging in Mice. *Foods*. 2024;**13**(13). [PubMed ID: 38998477]. [PubMed Central ID: PMC11241504]. <https://doi.org/10.3390/foods13131971>.
27. Luna LG. *Histopathologic Methods and Color Atlas of Special Stains and Tissue Artifacts*. American Histolabs;1992.
28. Bradford MM. A rapid and sensitive method for the quantitation of microgram quantities of protein utilizing the principle of protein-dye binding. *Anal Biochem*. 1976;**72**:248-54. [PubMed ID: 942051]. [https://doi.org/10.1016/0003-2697\(76\)90527-3](https://doi.org/10.1016/0003-2697(76)90527-3).
29. Ellman GL. Tissue sulfhydryl groups. *Arch Biochem Biophys*. 1959;**82**(1):70-7. [PubMed ID: 13650640]. [https://doi.org/10.1016/0003-9861\(59\)90090-6](https://doi.org/10.1016/0003-9861(59)90090-6).
30. Iwata M, Corn T, Iwata S, Everett MA, Fuller BB. The relationship between tyrosinase activity and skin color in human foreskins. *J Invest Dermatol*. 1990;**95**(1):9-15. [PubMed ID: 1973189]. <https://doi.org/10.1111/1523-1747.ep12872677>.
31. Talwar HS, Griffiths CE, Fisher GJ, Russman A, Krach K, Benrazavi S, et al. Differential regulation of tyrosinase activity in skin of white and black individuals in vivo by topical retinoic acid. *J Invest Dermatol*. 1993;**100**(6):800-5. [PubMed ID: 8496619]. <https://doi.org/10.1111/1523-1747.ep12476615>.
32. Sirerol JA, Feddi F, Mena S, Rodriguez ML, Sirera P, Aupi M, et al. Topical treatment with pterostilbene, a natural phytoalexin, effectively protects hairless mice against UVB radiation-induced skin

- damage and carcinogenesis. *Free Radic Biol Med*. 2015;**85**:1-11. [PubMed ID: 25845487]. <https://doi.org/10.1016/j.freeradbiomed.2015.03.027>.
33. Ittycheri A, Lipsky ZW, Hookway TA, German GK. Ultraviolet light induces mechanical and structural changes in full thickness human skin. *J Mech Behav Biomed Mater*. 2023;**143**:105880. [PubMed ID: 37172426]. <https://doi.org/10.1016/j.jmbbm.2023.105880>.
34. Cho S, Lee DH, Won CH, Kim SM, Lee S, Lee MJ, et al. Differential effects of low-dose and high-dose beta-carotene supplementation on the signs of photoaging and type I procollagen gene expression in human skin in vivo. *Dermatology*. 2010;**221**(2):160-71. [PubMed ID: 20516658]. <https://doi.org/10.1159/000305548>.
35. Ighodaro OM, Akinloye OA. First line defence antioxidants-superoxide dismutase (SOD), catalase (CAT) and glutathione peroxidase (GPX): Their fundamental role in the entire antioxidant defence grid. *Alexandria J Med*. 2019;**54**(4):287-93. <https://doi.org/10.1016/j.ajme.2017.09.001>.
36. Matuz-Mares D, Riveros-Rosas H, Vilchis-Landeros MM, Vazquez-Meza H. Glutathione Participation in the Prevention of Cardiovascular Diseases. *Antioxidants (Basel)*. 2021;**10**(8). [PubMed ID: 34439468]. [PubMed Central ID: PMC8389000]. <https://doi.org/10.3390/antiox10081220>.
37. Brenner M, Hearing VJ. The protective role of melanin against UV damage in human skin. *Photochem Photobiol*. 2008;**84**(3):539-49. [PubMed ID: 18435612]. [PubMed Central ID: PMC2671032]. <https://doi.org/10.1111/j.1751-1097.2007.00226.x>.
38. Moon KM, Lee MK, Park SY, Seo J, Kim AR, Lee B. Docosatrienoic Acid Inhibits Melanogenesis Partly through Suppressing the Intracellular MITF/Tyrosinase Axis. *Pharmaceuticals (Basel)*. 2024;**17**(9). [PubMed ID: 39338360]. [PubMed Central ID: PMC11435182]. <https://doi.org/10.3390/ph17091198>.
39. Kaminski K, Kazimierczak U, Kolenda T. Oxidative stress in melanogenesis and melanoma development. *Contemp Oncol (Pozn)*. 2022;**26**(1):1-7. [PubMed ID: 35506034]. [PubMed Central ID: PMC9052339]. <https://doi.org/10.5114/wo.2021.112447>.
40. Jenkins NC, Grossman D. Role of melanin in melanocyte dysregulation of reactive oxygen species. *Biomed Res Int*. 2013;**2013**:908797. [PubMed ID: 23555101]. [PubMed Central ID: PMC3600250]. <https://doi.org/10.1155/2013/908797>.